Ultrasound in Med. & Biol., Vol. 47, No. 6, pp. 1586–1595, 2021

0301-5629/$ - see front matter

https://doi.org/10.1016/j.ultrasmedbio.2021.02.009

● *Original Contribution*

LOW-INTENSITY PULSED ULTRASOUND PROMPTS BOTH FUNCTIONAL AND HISTOLOGIC IMPROVEMENTS WHILE UPREGULATING THE BRAIN-DERIVED NEUROTROPHIC FACTOR EXPRESSION AFTER SCIATIC CRUSH INJURY IN RATS

TIANSHU WANG,* AKIRA ITO,† SHIXUAN XU,† HIDEKI KAWAI,† HIROSHI KUROKI,† and TOMOKI AOYAMA*

* Department of Development and Rehabilitation of Motor Function, Human Health Sciences, Graduate School of Medicine, Kyoto University, Kyoto, Japan; and † Department of Motor Function Analysis, Human Health Sciences, Graduate School of Medicine, Kyoto University, Kyoto, Japan

(*Received* 16 *September* 2020; *revised* 22 *January* 2021; *in final from* 15 *February* 2021)

Abstract—The aim of this study was to determine that low-intensity pulsed ultrasound (LIPUS) at an intensity of 140 mW/cm^2 promotes functional and histologic improvements in sciatic nerve crush injury in a rat model and to investigate changes over time in relevant growth factors and receptors, exploring the mechanism of LIPUS in the recovery process after injury. Toe angle in the toe-off phase, regenerative axonal length, myelinated nerve fiber density, diameter of myelinated nerve fiber, axon diameter and myelin sheath thickness were significantly higher in the LIPUS group than in the sham group. Gene and protein expression of brain-derived neurotrophic factor (BDNF) was upregulated in the LIPUS group. In conclusion, LIPUS contributed to rapid functional and histologic improvement and upregulated BDNF expression after sciatic nerve crush injury in rats. (E-mail: ito.akira.4m@kyoto-u.ac.jp)

Key Words: **Low-intensity pulsed ultrasound, Peripheral nerve regeneration, Functional improvement, Changes over time, Brain-derived neurotrophic factor.**

INTRODUCTION

Peripheral nerve injury occurs in daily life because of mechanical damage resulting from bone fracture, muscle strains and prolonged sitting or lying with local pressure (Sun et al. 2009; Ni et al. 2017). Fortunately, these nerves can spontaneously repair through intrinsic regenerative capabilities (Gu et al. 2011); they undergo Wallerian degeneration, axonal regrowth, remyelination, axonal enlargement and functional re-innervation to achieve recovery (Menorca et al. 2013). Meanwhile, multiple growth factors and relevant receptors accompanied by proliferation and differentiation of participant cells, including Schwann cells, fibroblasts and macrophages, cause various regulated changes in gene or protein expression over time (Caillaud et al. 2019) and play a great role in the recovery of peripheral nerves after injury. However, the process of nerve regeneration is too slow for injured nerves to recover in a timely manner, which may cause temporary or long-term neuronal dysfunction, ultimately resulting in a deteriorating quality of life and a vast economic and social burden (Gu et al. 2011; Ni et al. 2017). Therefore, effective therapeutic measures to promote the process of peripheral nerve regeneration are necessary.

In recent years, various therapeutic methods have been used to improve peripheral nerve recovery using lasers (de Oliveira Rosso et al. 2018), electricity (Willand et al. 2016), shock waves (Schuh et al. 2016) and ultrasound (Sato et al. 2016). Low-intensity pulsed ultrasound (LIPUS) has been recognized as an efficient physical stimulus. Compared with common therapeutic ultrasound or other physical agents, it is low cost and non-invasive and does not cause any pain or discomfort during the treatment. LIPUS was first introduced to improve bone healing and soft tissues such as tendons and ligaments (Handolin et al. 2002; Warden 2003; Khanna et al. 2009). Recent *in vivo* and *in vitro* studies have revealed that LIPUS accelerates the process of peripheral nerve regeneration (Crisci and Ferreira 2002; Chang et al. 2005; Zhang et al. 2009; Jiang et al. 2016; Ito et al. 2020). The intensity varied among numerous studies; although each was considered definitely

Address correspondence to: Akira Ito, 53 Shogoin, Kawahara-cho, Sakyo-ku, Kyoto 606-8507, Japan. E-mail: ito.akira.4m@kyoto-u.ac.jp

effective (Zhang et al. 2009; Jiang et al. 2016; Sato et al. 2016; Zhao et al. 2016; Xia et al. 2019), the optimal intensity of LIPUS remains unclear. Moreover, the effect of LIPUS stimulation on changes over time in gene or protein expression of growth factors remains unrevealed.

Our previous study reported that compared with that at an intensity of 30 or 250 mW/cm^2, LIPUS stimulation, at an intensity (spatial average temporal average, SATA) of 140 mW/cm^2 maximally promoted nerve regeneration in a rat model of sciatic nerve crush injury (Ito et al. 2020). Nevertheless, according to the results of functional assessments using the sciatic functional index (SFI) (Ito et al. 2020), obvious functional improvements were not detected, and the results of histologic analyses were required to supplement and firmly support the conclusion.

Therefore, the aim of this study was to determine that LIPUS at an intensity of 140 mW/cm^2 promotes both functional and histologic improvements in a rat model of sciatic nerve crush injury. We also wanted to investigate changes in gene and protein expression of relevant growth factors and receptors markedly affected by LIPUS, to reveal the mechanism underlying the recovery process after sciatic nerve injury.

METHODS

Twelve-week-old male Lewis rats (weight: 280−310 g) were housed in groups of three per cage on a 12-h light-dark cycle and fed commercial rat food and tap water *ad libitum*. The rats (n = 18) were randomly and equally assigned to two groups: sham (n = 9) and LIPUS (n = 9). Functional evaluations and histomorphometric analyses were performed 20 and 30 d after surgery, respectively. In addition, three normal rats housed only for functional evaluations constituted the intact group. On the other hand, another array of rats was divided into four groups based on different time points after surgery: 3, 7, 14 and 30 d (n = 18 for each group). The rats in each group were subdivided into the sham (n = 9) and LIPUS (n = 9) groups as well; real-time polymerase chain reaction (PCR) (n = 6 for each subdivided group) and immunofluorescence staining (n = 3 for each subdivided group) were performed in each group at various time points. This study was approved by the Animal Experimentation Committee of Kyoto University, and all experiments were performed in accordance with the Guidelines of the Animal Experimentation Committee, Kyoto University (Approval No. MedKyo20027).

Surgery

A crush injury was created in the left sciatic nerve according to a previously described protocol (Wang et al. 2018) while the rat was anesthetized using an intraperitoneal injection of a combination anesthetic prepared with 0.15 mg/kg medetomidine hydrochloride, 2 mg/kg midazolam and 2.5 mg/kg butorphanol tartrate. Briefly, the sciatic nerve was exposed with a lateral longitudinal straight incision from the greater trochanter to midthigh, and a 2-mm-long crush injury was created at the site directly below the gluteal tuberosity using a standard surgical hemostat. The proximal end of the injury was marked using a stereomicroscope (Leica, Heidelberg, Germany) with a single 9-O nylon (BEAR Medical Inc., Tokyo, Japan) epineural stitch. The muscle and skin were then closed with 4-O nylon sutures.

LIPUS protocol

LIPUS treatment was implemented on the first day after surgery, modifying a previously reported study (Jiang et al. 2016). All rats were anesthetized with 2% isoflurane inhalation solution and placed in the right lateral position. The LIPUS transmission gel was applied before placing the transducer on the injury site of the skin. Stimulation was performed using a portable ultrasonic treatment apparatus and an affiliated circular ultrasonic probe with an effective radiation area of 0.9 cm^2 and a 2.9 beam non-uniformity ratio (UST-770, ITO Physiotherapy & Rehabilitation, Tokyo, Japan). The LIPUS parameters were as follows: 1-MHz acoustic frequency, 1-kHz pulsed repeating frequency, 20% duty cycle, and 5 min/d duration; intensities were 0 and 140 mW/cm^2 (SATA) for rats in the sham and LIPUS groups, respectively. The rats received LIPUS treatment daily until the 14th day the surgery and then 5 d/wk until death.

Kinematic analysis

To evaluate functional recovery, a 3-D motion capture apparatus consisting of a treadmill, four 120-Hz charged coupled device cameras and data processing software (Kinema Tracer System, Kissei Comtec, Nagano, Japan) was used. Before walking on the treadmill, rats were equipped with markers under anesthesia according to our previously described procedure (Wang et al. 2020). Colored hemispheric markers were bilaterally adhered to five landmarks: the anterior superior iliac spine, greater trochanter, knee joint, lateral malleolus and fifth metatarsophalangeal joint. The tip of the fourth toe was marked with pink ink (paint marker, Nippon Paint Co., Ltd, Tokyo, Japan). After a calibration process, hindlimb motions were recorded with charged coupled device cameras while the rats were walking on the treadmill. For subsequent analysis, 10 consecutive steps were recorded from each rat, and the affiliated software automatically built 3-D kinematic models and processed data based on tracing markers attached to the landmarks (Wang et al. 2018). In this study, two joint angles were measured. The ankle angle was the angle formed by a line connecting the knee joint and lateral

malleolus and another line connecting the lateral malleolus and the fifth metatarsophalangeal joint. The toe angle was formed by a line connecting the fifth metatarsophalangeal joint and the tip of the fourth toe and another extension line from the lateral malleolus to the fifth metatarsophalangeal joint. The degree of toe angle at dorsiflexion was denoted as plus, and that at plantarflexion was conversely denoted as minus. Moreover, joint angles in the toe-off phase were measured by referring to our previous study (Wang et al. 2018). The joint angle of each rat was the mean angle recorded from 10 recorded walking steps. The joint trajectory was the mean curve composed of the joint angles in the normalized step cycle of all the rats in a group, and the joint angle in the toe-off phase was the mean angle composed of the joint angles in the toe-off phase of all the rats in a group.

Histomorphometric analysis

Thirty days after surgery, after animal euthanasia, a 5-mm-long sciatic nerve specimen was dissected from the epineural stitch and then immersed in a fixative containing 1.44% paraformaldehyde and 1% glutaraldehyde in 0.036 M phosphate buffer (pH 6.8) at 4˚C overnight. Subsequently, according to our previously described protocol (Wang et al. 2018), the specimen was fixed with 1% osmium tetroxide in 0.1 M phosphate buffer for 120 min and then dehydrated through graded ethanol aqueous solutions and finally in 100% ethanol. Afterward, the dehydrated specimen was embedded in EPON (Luveak, Nacalai Teque, Kyoto, Japan). Transverse sections (1 μm thick) were prepared and stained with toluidine blue solution, then images were captured at 200 × magnification using a light microscope (ECLIPSE 80 i, Nikon, Tokyo, Japan). The myelinated nerve fibers were counted in random areas of 90,000 μm^2, accounting for not less than 30% of the total area of an image using ImageJ (National Institutes of Health, Bethesda, MD, USA). The result was denoted as myelinated nerve fiber density, representing the mean number of myelinated nerve fibers in three of the above-mentioned areas.

Ultrathin transverse sections of the same tissue stained with uranyl acetate and lead citrate were also examined under a transmission electron microscope (Model H-7000, Hitachi High-Technologies, Tokyo, Japan). Ten pictures representing random areas of the section were obtained at 2000 × magnification, and the shortest diameter of myelinated nerve fiber (α) and axon diameter (β) of each myelinated nerve fiber was measured. The myelin sheath thickness of each myelinated nerve fiber was calculated according to the formula $(\alpha - \beta)/2$. Averages of these three parameters from all myelinated nerve fibers were regarded as the mean diameter of myelinated nerve fiber, mean axon diameter and mean thickness of the myelin sheath, respectively.

Quantitative real-time PCR

A 10-mm-long sciatic nerve was dissected from the epineural stitch of each rat, and four normal sciatic nerves on the contralateral side, as long as the one on the injured side, were likewise dissected as an intact group. Total RNA was extracted from the sciatic nerve specimens using the RNeasy Plus Universal Mini Kit (Qiagen, Valencia, CA, USA) and then tested for purity using the NanoDrop2000 (Thermo Fisher Scientific, Wilmington, DE, USA). The A_{260}/A_{280} ratios for all specimens were >2. Next, 1 μg of total RNA was reverse-transcribed into complementary DNA, and TaqMan gene expression assays were used for brain-derived neurotrophic factor (BDNF), nerve growth factor (NGF), low-affinity NGF receptor (NGFR) and vascular endothelial growth factor A (VEGFA). Quantitative real-time PCR was then performed using an Applied Biosystems 7500 Real-Time PCR System (Applied Biosystems, Foster City, CA, USA). Standard enzyme and cycling conditions for the 7500 Real-Time PCR System were utilized, and glyceraldehyde 3-phosphate dehydrogenase was used as the endogenous reference gene because of its high stability under these study conditions.

The data obtained were analyzed using the comparative threshold cycle method. The amount of target gene was normalized to that of glyceraldehyde 3-phosphate dehydrogenase. The value of the calibration specimens (specimens in the intact group) was set to 1, and the values of specimens in the sham and LIPUS groups at different time points after surgery were represented relative to that of the calibration specimens (Ito et al. 2020).

Immunohistochemistry

An approximately 8-mm-long sciatic nerve was dissected from the epineural stitch of each rat. After fixation with 4% paraformaldehyde and cryoprotection with 30% sucrose, 10-μm-thick cryostat longitudinal sections were prepared. Next, after rinsing with phosphate-buffered saline (PBS), blocking buffer containing 5% goat serum was added to the slides for an hour-long incubation at room temperature. Rabbit anti-BDNF primary antibody (1:200, Bioss Inc., Woburn, MA, USA) was then applied, and the slides were incubated overnight at 4˚C. The slides were then rinsed with PBS and Alexa Fluor 488 goat anti-rabbit IgG (1:200, Thermo Fisher Scientific, Waltham, MA, USA), and a secondary antibody was applied for 2 h at room temperature. After rinsing with PBS, the same blocking solution was applied followed by rabbit anti-Neurofilament-L antibody (Alexa Fluor 594 conjugate, 1:200, Cell Signaling Technology, Danvers, MA, USA) for 24 h at 4˚C. After final PBS washes, coverslips were mounted on all slides using an aqueous mounting medium. For sections labeled for Neurofilament-L, images of axonal outgrowth were

captured using a macro zoom microscope (MVX10, Olympus, Shinjuko, Japan). The regenerative axonal length was measured using ImageJ. For the BDNF sections, images of the crush injury site (crush site) and the site 5 mm distal to the epineural stitch (distal) were obtained with a confocal laser scanning microscope (FV10 i, Olympus).

Statistical analysis

Data are expressed as the mean ± standard deviation. Student's *t*-test was used for comparisons between sham and LIPUS groups, and Dunnett's test was used for comparison between each group and the intact group. Statistical significance was indicated by a p value <0.05.

RESULTS

LIPUS accelerated sciatic functional improvement

Compared with the intact group, the results indicated that the joint trajectory of neither the sham nor the LIPUS group returned to normal. The joint trajectory of the sham group, in the step cycle period, had a striking similarity to that of the LIPUS group, in the ankle and toe angle. The ankle trajectory of the sham group was lower than that of the LIPUS group, but the gap between them was small, especially in the swing phase (Fig. 1a). Nevertheless, not only was the toe trajectory of the sham group much lower, but it also extended the gap between the groups (Fig. 1b). To compare the joint angles between both groups, the joint angles in the toe-off phase were calculated. The results revealed that although there was no significant difference between the sham and LIPUS groups in the ankle angle, the toe angle of the LIPUS group was significantly higher than that of the sham group (Fig. 1c).

LIPUS promoted nerve regeneration

Axonal outgrowths were not found 3 and 7 d after surgery (Fig. 2a, 2b). However, prominent axonal outgrowths were found at 14 d (Fig. 2c), and their length further increased 30 d after surgery (Fig. 2d), in both sham and LIPUS groups. Quantitative analysis revealed that regenerative axonal length was significantly higher in the LIPUS group than in the sham group 14 d after surgery (Fig. 2e). Regenerative axonal lengths 30 d after surgery in both groups were beyond the range of measurement.

Representative images of the transected sciatic nerve processed with toluidine blue staining are provided in Figure 3a. Quantitative analysis indicated that the myelinated nerve fiber density significantly increased in the LIPUS group compared with the sham group (Fig. 3b).

Representative images of the transected sciatic nerve obtained by transmission electron microscopy are provided as well. Thin and thick myelinated nerve fibers coexisted in the sham group, while myelinated nerve fibers in the LIPUS group presented uniform amplification (Fig. 4a). Quantitative analysis also proved that myelinated nerve fiber diameter, axon diameter or myelin sheath thickness was significantly greater in the LIPUS group than in the sham group (Fig. 4b, 4d).

LIPUS regulated gene expression of relevant growth factors and receptor

Compared with that of the intact group, mRNA expression of BDNF in the LIPUS group was significantly upregulated 14 and 30 d after surgery, although that in the sham group was only upregulated 14 d after surgery (Fig. 5a). mRNA NGF was significantly overexpressed in both groups 7 d after surgery (Fig. 5b). mRNA NGFR expression was significantly upregulated at 3 and 7 d, in both groups, but decreased to an insignificant level 14 d after surgery in the LIPUS group (Fig. 5c). mRNA expression of VEGFA was significantly upregulated only in the sham group 7 d after surgery (Fig. 5d). However, there was no difference in gene expression between sham and LIPUS groups at any time point.

LIPUS elevated protein expression of BDNF

Protein expression of BDNF reached a peak 7 d after surgery, rapidly decreased on the crush injury site, and no evident or minute expression was found in the distal part of the sham group. Protein expression of BDNF rapidly reached a peak at 3 d and maintained a fairly high level until 30 d after injury on the crush injury site in the LIPUS

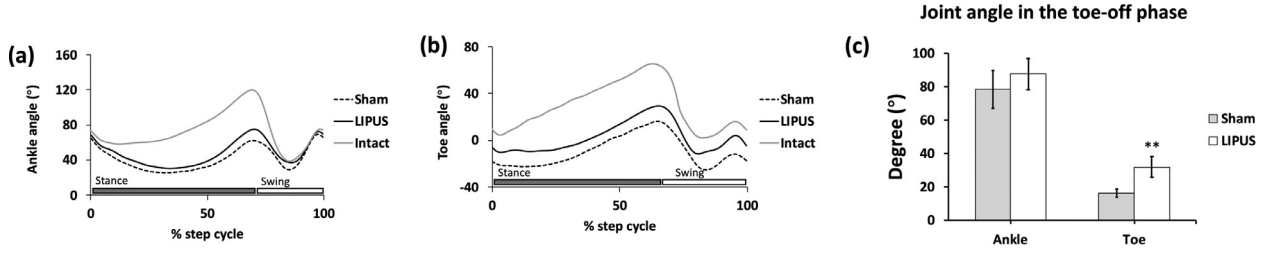

Fig. 1. Time course trajectories of joint angles. (a) Changes in ankle angle in a step cycle. (b) Changes in toe angle in a step cycle. (c) Ankle and toe angles in the toe-off phase. *$p < 0.01$, compared with the sham group. LIPUS = low-intensity pulsed ultrasound.

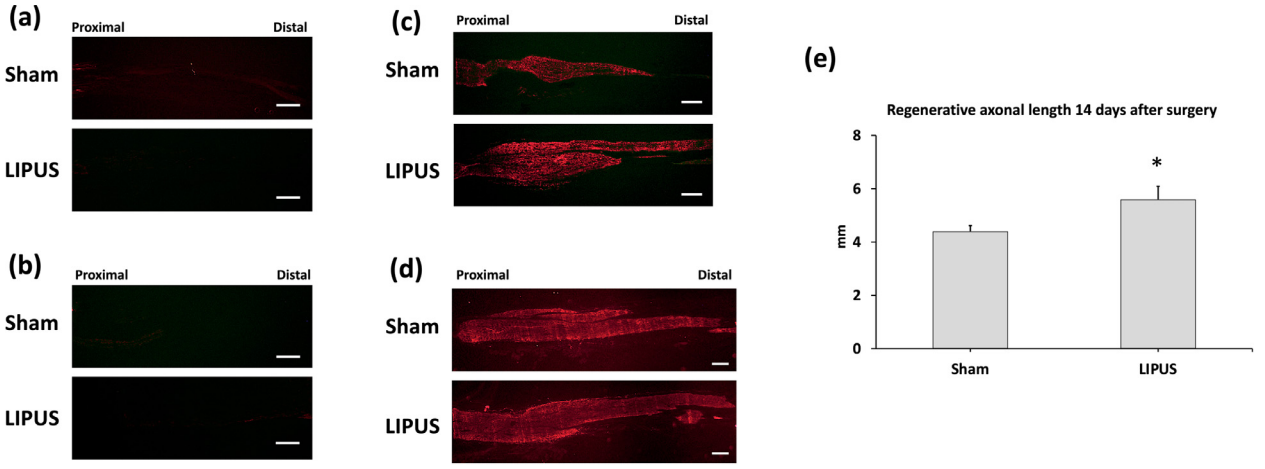

Fig. 2. Immunohistochemistry of sciatic nerve (a) 3, (b) 7, (c) 14 and (d) 30 d after surgery. Longitudinal sections of sciatic nerves were labeled for Neurofilament-L (*red*) (scale bars = 500 μm). Axons were not detected at 3 and 7 d, and regenerative axons were observed 14 and 30 d after injury. (e) Regenerative axonal length 14 d after surgery. *$p < 0.05$, compared with the sham group. LIPUS = low-intensity pulsed ultrasound.

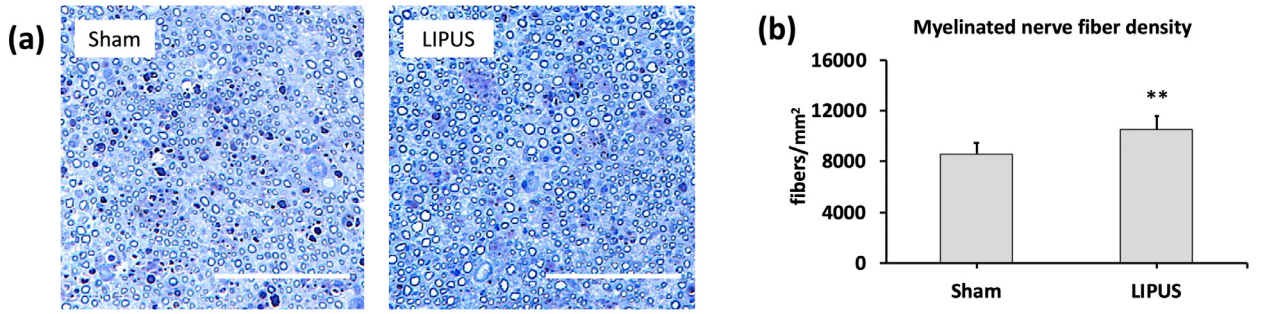

Fig. 3. Myelinated nerve fiber density. (a) Representative images of transected sciatic nerve stained with toluidine blue (scale bars = 100 μm). (b) Mean myelinated nerve fiber density. *$p < 0.01$, compared with the sham group. LIPUS = low-intensity pulsed ultrasound.

group. Moreover, noteworthy protein expression of BDNF was also detected in the distal part from 7 to 30 d after injury, although it slowly decreased (Fig. 6).

DISCUSSION

In this study, we investigated the effect of LIPUS on functional recovery and regeneration of the rat sciatic nerve after a crush injury. Moreover, we explored the changes in gene expression of relevant growth factors and receptor and protein expression of BDNF, as well as axonal outgrowth, at multiple time points after injury, to clarify the mechanism underlying LIPUS. Jiang et al. (2016) found that although LIPUS at 500 or 750 mW/cm^2 was able to induce nerve regeneration, 250 mW/cm^2 significantly induced the most rapid regeneration. In contrast, several studies have reported that the intensity of ultrasound should be regulated below 500 mW/cm^2, and high-intensity (>500 mW/cm^2) ultrasound may cause cell injury and impede tissue recovery (Ahmadi et al. 2012; Zhong et al. 2013; Lee et al. 2014). Moreover, low-intensity ultrasound (30−50 mW/cm^2) has been verified to be sufficiently effective in enhancing nerve growth and accelerating nerve regeneration (Sato et al. 2016; Zhao et al. 2016). Therefore, choosing an optimal intensity of LIPUS is the primary element in this study. Our previous study determined that LIPUS at an intensity of 140 mW/cm^2 might be an optimum option because it is considered moderate and harmless to the sciatic nerve and propelled axonal regrowth and remyelination more than LIPUS at an intensity of 30 or 250 mW/cm^2 (Ito et al. 2020). Other parameters of LIPUS, except intensity, were set based on the most effective scheme introduced by Akhlaghi et al. (2012).

We conducted a kinematic analysis with a 3-D motion capture apparatus to evaluate sciatic functional recovery instead of the traditional SFI (Ito et al. 2019). In addition to the SFI with its intrinsic shortcomings (Walker et al. 1994),

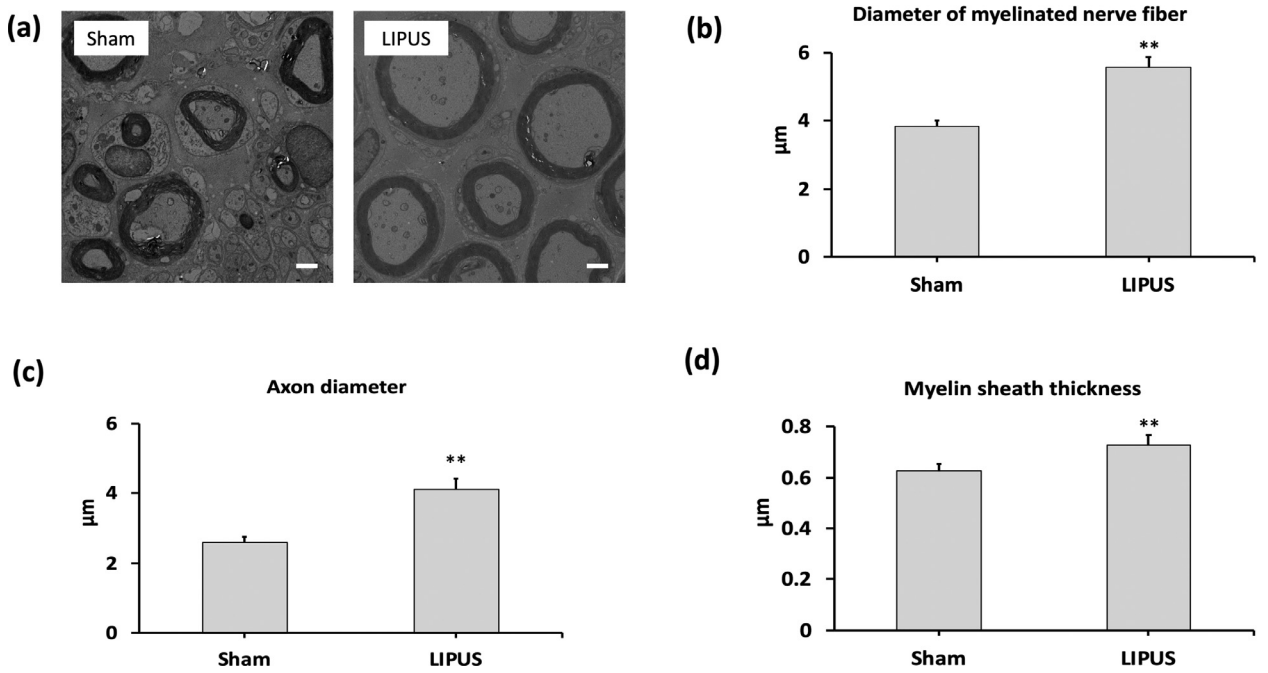

Fig. 4. Transmission electron micrographs of transected sciatic nerve. (a) Representative transmission electron micrographs of transected sciatic nerve (scale bars = 2 μm). (b) Mean myelinated nerve fiber diameter, (c) axon diameter and (d) myelin sheath thickness. *$p < 0.01$, compared with the sham group. LIPUS = low-intensity pulsed ultrasound.

kinematic analysis is also recognized as a sensitive and accurate method for functional evaluation (de Ruiter et al. 2007). Although there was no obvious difference in the ankle angle between the sham and LIPUS groups, the toe angle in the LIPUS group quickly improved compared with that in the sham group. This result indicated that marked functional reinnervation resulted from LIPUS stimulation because our previous study had verified that the toe angle is a reliable and an accurate parameter in the kinematic analysis (Wang et al. 2018), and the toe angle had greater sensitivity than the ankle angle, which corresponds to the conclusions of previous studies (Tajino et al. 2018; Wang et al. 2018). With respect to histomorphometric results, we found that myelinated nerve fiber density, the diameter of myelinated nerve fiber, axon diameter and myelin sheath thickness were higher in the LIPUS group than in the sham group. In addition, immunohistochemistry results revealed that regenerative axonal length was significantly longer in the LIPUS group than in the sham group 14 d after injury. Regenerative axonal lengths 30 d after surgery in both groups exceeded the length of dissected sciatic nerves, and the regenerative axons had already innervated end-organs 30 d after surgery (Wang et al. 2018); thus, regenerative axonal lengths were beyond the range of measurement. These results indicated that LIPUS stimulation not only accelerated axonal regrowth but also promoted remyelination and axonal enlargement to induce more mature myelinated nerve fibers.

Application of LIPUS to peripheral nerve regeneration revealed mechanical effects resulting from acoustic pressure waves, accompanied by extremely low heating effects (Khanna et al. 2009). A previous review also reported that the micromechanical stimulation induced by LIPUS played an important role (Romano et al. 2009). Micromechanical stimulation may whet enzyme activity and modify cell metabolism, subsequently promoting the synthesis of relevant cytokines and growth factors, while guiding multiple cellular responses, including cellular migration, proliferation and differentiation (Dunn and Olmedo 2016). In the peripheral nervous system, micromechanical stimulation derived from LIPUS transmits signals *via* integrin acting as a mechanoreceptor on the cell membrane, and focal adhesion kinase is then phosphorylated to initiate signal transduction *via* the phosphatidylinositol 3-OH kinase /Akt or glycogen synthase kinase 3β (GSK-3β)/β-catenin pathway. On the other hand, micromechanical stress may activate the stretch-activated ion channels on the cell membrane, triggering the downstream extracellular signal-regulated protein kinase (ERK1/2)/cyclic adenosine monophosphate-regulated enhancer B (CREB) pathway (Zhao et al. 2016; Ren et al. 2018; Peng et al. 2020). Ultimately, a series of intracellular reactions are activated, thereby elevating the expression of neurotrophic factors and receptors, including BDNF, NGF, VEGFA and NGFR, and promoting Schwann cell proliferation,

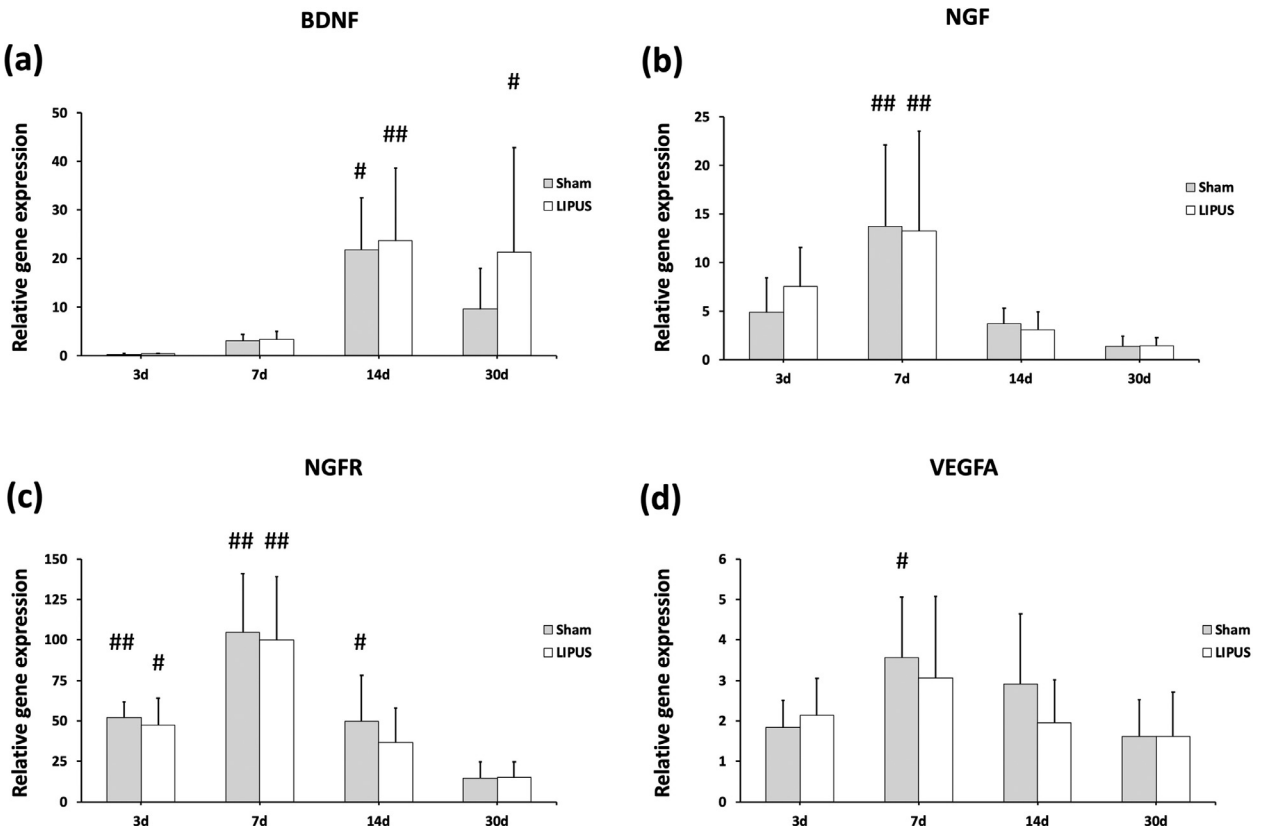

Fig. 5. Gene expression analysis 3, 7, 14 and 30 d after surgery. Gene expression of (a) BDNF, (b) NGF, (c) NGFR and (d) VEGFA in the sham and LIPUS groups. The value of the calibration sample (intact nerve specimen; n = 4) was set as 1. $^{*}p < 0.05$, $^{\dagger}p < 0.01$, compared with the calibration sample. BDNF = brain-derived neurotrophic factor; LIPUS = low-intensity pulsed ultrasound; NGF = nerve growth factor; NGFR = low-affinity NGF receptor; VEGFA = vascular endothelial growth factor A.

cell survival and neurite outgrowth (Su et al. 2017; Peng et al. 2020; Shindo and Shimokawa 2020).

Neurotrophic factors are essential for controlling the survival, proliferation and differentiation of neural and non-neural cells involved in nerve regeneration (Hausner and Nógrádi 2013). BDNF is well known to promote axonal sprouting and myelinogenesis (Chan et al. 2001; Gordon 2009). Removal of BDNF not only impedes the increase in nerve fibers, especially medullated fibers, but also inhibits myelination *in vitro* and *in vivo* (Cosgaya et al. 2002). Hence, BDNF is an exceedingly important neurotrophic factor and plays an indispensable role in peripheral nerve recovery after injury. Our study indicated that gene expression of BDNF in the sham group arose at 7 d, notably increased by 14 d and subsequently decreased 30 d after injury. This process was roughly consistent with a previous finding (Pan et al. 2017). However, the gene expression of BDNF in the LIPUS group was maintained at a high level until 30 d, in the wake of significant upregulation 14 d after injury. This finding suggested that gene expression of BDNF was intensely affected by LIPUS and thereby was maintained for a longer time after upregulation. On the other hand, immunohistochemistry results indicated much stronger protein expression of BDNF at the crush and distal sites in the LIPUS group, suggesting that the mechanical stimulation generated by LIPUS resulted in the upregulation and maintenance of BDNF protein expression. It is worth mentioning that not only at the crush injury site, protein expression also exhibited intense upregulation and persistence without precedent on the distal part of the rat sciatic nerve stimulated by LIPUS.

NGFR is expressed mainly in the distal part of the nerve after injury, and its induction has been proposed as a mechanism to concentrate neurotrophic factors, including NGF and BDNF, recruit the ligand and thereby promote nerve regeneration (Johnson et al. 1988). VEGFA plays a crucial role in local angiogenesis, triggering peripheral nerve regeneration in the very early stages after nerve injury (Nishida et al. 2018). Our study found that mRNA expression of NGFR was significantly overexpressed from 3 to 14 d and peaked 7 d after injury, and that of VEGFA was significantly overexpressed only at 7 d after injury during the spontaneous nerve recovery process, while immunohistochemistry analysis implied that the Wallerian degeneration

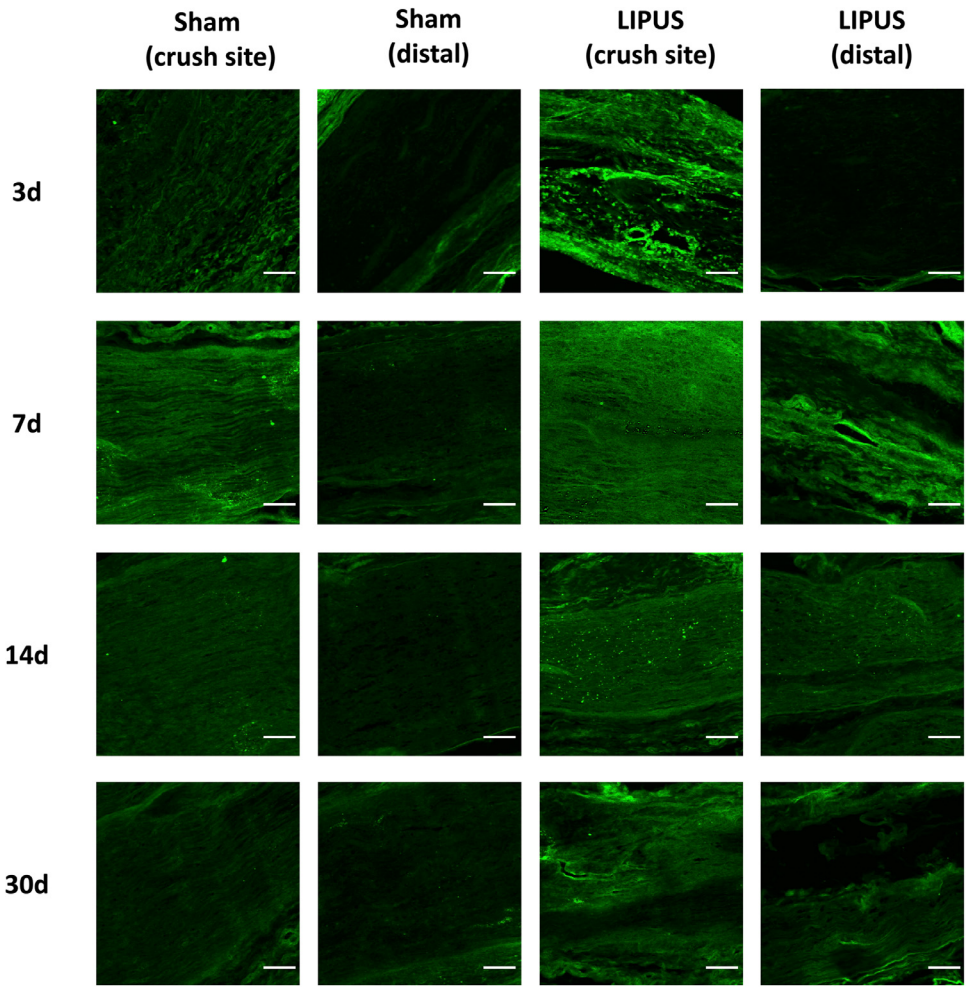

Fig. 6. Immunohistochemistry of sciatic nerve 3, 7, 14 and 30 d after surgery. Longitudinal sections of sciatic nerves were labeled for brain-derived neurotrophic factor (*green*) (scale bars = 100 μm).

persisted without any axonal outgrowth at least until 7 d after injury in both groups. These findings indicated that mRNA expression of NGFR and VEGFA was upregulated during Wallerian generation and gradually downregulated after axonal outgrowth. Therefore, with respect to the mechanism underlying LIPUS, a reasonable explanation is that LIPUS stimulation perhaps accelerated the process of Wallerian degeneration, thereby resulting in no noteworthy gene expression of NGFR and VEGFA 14 and 7 d after injury, respectively. In addition, NGF promotes the proliferation and differentiation of neurons and repairs injured nerves (Petruska and Mendell 2004; Unezaki et al. 2009). A previous study reported that upregulated NGF results in Schwann cell differentiation and proliferation in anticipation of the arrival of axonal outgrowth (Campbell 2008), as observed in our findings on significant overexpression of NGF in both the sham and LIPUS groups 7 d after injury. Nevertheless, there was no obvious expression in either group 3, 14 or 30 d after injury, indicating that gene expression of NGF was not regulated by LIPUS, and overexpression of NGF appeared only in the middle and terminal phases of Wallerian degeneration.

Several limitations cannot be overlooked in this study. The small sample size in the real-time PCR analysis might have resulted in the detection of no significant difference between sham and LIPUS groups. The sciatic nerve is a mixed nerve composed of motor and sensory fibers, and to realize functional and efficient movements, feedback from sensory fibers is necessary; however, the effects of LIPUS on regenerated sensory fibers and sensory function were not investigated. Although mechanical stimulation is the greatest effect of LIPUS, the low heating effect might still cause tiny variations in several temperature-sensitive enzyme activities, thereby eliciting unknown effects on peripheral nerve recovery after injury (Khanna et al. 2009). Moreover, protein expression of NGFR and VEGFA was not investigated, because gene expression of NGFR and VEGFR was not

markedly affected by LIPUS. Investigating their protein expression would help to justify our assumption: LIPUS stimulation shortens the process of Wallerian degeneration, thereby accelerating nerve generation. Multiple other neurotrophic factors and receptors participate in Wallerian degeneration and nerve regeneration as well, but changes in their gene or protein expression over time have not yet been discovered. Further studies are expected to solve these problems, thus sufficiently and thoroughly increasing the understanding of the mechanisms underlying LIPUS in the recovery process after peripheral nerve injury.

Nevertheless, LIPUS is still expected to be a useful therapeutic method for repair of damaged peripheral nerve tissues in future clinical applications. Moreover, given its non-invasiveness, biological tolerability and positive effects on Schwann cells, LIPUS may be a seminal therapeutic option in rehabilitation after peripheral nerve reconstruction, microsurgery and even transplantation with Schwann cells. We believe that LIPUS can exhibit extraordinary abilities in the emerging field of regenerative rehabilitation (Willett et al. 2020), in the wake of more clinical research focusing on LIPUS.

In conclusion, both gene and protein expression of BDNF was upregulated by LIPUS, and the particularly notable elevated expression of BDNF at the site distal to the injury might play a greater role in rapidly promoting both functional and histologic improvements after sciatic nerve crush injury in rats.

Acknowledgments—We thank Keiko Okamoto Furuta and Haruyasu Kouda (Division of Electron Microscopic Study, Center for Anatomical Studies, Graduate School of Medicine, Kyoto University, Kyoto) for their technical assistance with electron microscopy. We also thank Editage (www.editage.com) for English language editing.

Conflict of interest disclosure—The authors have no conflicts of interest to declare. All co-authors have seen and agree with the contents of the article, and there is no financial interest to report. We certify that the submission is original work and is not under review at any other publication.

REFERENCES

Ahmadi F, McLoughlin IV, Chauhan S, ter-Haar G. Bio-effects and safety of low-intensity, low-frequency ultrasonic exposure. Prog Biophys Mol Biol 2012;108:119–138.

Akhlaghi Z, Mobarakeh JI, Mokhtari M, Behnam H, Rahimi AA, Khajeh Hosseini MS, Samiee F. The effects of altered ultrasound parameters on the recovery of sciatic nerve injury. Iran Biomed J 2012;16:107–112.

Caillaud M, Richard L, Vallat JM, Desmouliere A, Billet F. Peripheral nerve regeneration and intraneural revascularization. Neural Regen Res 2019;14:24–33.

Campbell WW. Evaluation and management of peripheral nerve injury. Clin Neurophysiol 2008;119:1951–1965.

Chan JR, Cosgaya JM, Wu YJ, Shooter EM. Neurotrophins are key mediators of the myelination program in the peripheral nervous system. Proc Natl Acad Sci USA 2001;98:14661–14668.

Chang CJ, Hsu SH, Lin FT, Chang H, Chang CS. Low-intensity-ultrasound-accelerated nerve regeneration using cell-seeded poly(D,L-lactic acid-co-glycolic acid) conduits: An in vivo and in vitro study. J Biomed Mater Res B Appl Biomater 2005;75:99–107.

Cosgaya JM, Chan JR, Shooter EM. The neurotrophin receptor $p75^{NTR}$ as a positive modulator of myelination. Science 2002;298:1245–1248.

Crisci AR, Ferreira AL. Low-intensity pulsed ultrasound accelerates the regeneration of the sciatic nerve after neurotomy in rats. Ultrasound Med Biol 2002;28:1335–1341.

de Oliveira Rosso MP, Buchaim DV, Kawano N, Furlanette G, Pomini KT, Buchaim RL. Photobiomodulation therapy (PBMT) in peripheral nerve regeneration: A systematic review. Bioengineering 2018;5:1–12.

de Ruiter GC, Spinner RJ, Alaid AO, Koch AJ, Wang H, Malessy MJA, Currier BL, Yaszemski MJ, Kaufman KR, Windebank AJ. Two-dimensional digital video ankle motion analysis for assessment of function in the rat sciatic nerve model. J Peripher Nerv Syst 2007;12:216–222.

Dunn SL, Olmedo ML. Mechanotransduction: Relevance to physical therapist practice—Understanding our ability to affect genetic expression through mechanical forces. Phys Ther 2016;96:712–721.

Gordon T. The role of neurotrophic factors in nerve regeneration. Neurosurg Focus 2009;26:E3.

Gu X, Ding F, Yang Y, Liu J. Construction of tissue engineered nerve grafts and their application in peripheral nerve regeneration. Prog Neurobiol 2011;93:204–230.

Handolin L, Pohjonen T, Partio EK, Arnala I, Tormala P, Rokkanen P. The effects of low-intensity pulsed ultrasound on bioabsorbable self-reinforced poly L-lactide screws. Biomaterials 2002;23:2733–2736.

Hausner T, Nógrádi A. The use of shock waves in peripheral nerve regeneration: New perspectives?. Int Rev Neurobiol 2013;109:85–98.

Ito A, Tianshu W, Tajino J. Three-dimensional motion analysis for evaluating motor function in rodents with peripheral nerve injury. Neural Regen Res 2019;14:2077–2078.

Ito A, Wang T, Nakahara R, Kawai H, Nishitani K, Aoyama T, Kuroki H. Ultrasound therapy with optimal intensity facilitates peripheral nerve regeneration in rats through suppression of pro-inflammatory and nerve growth inhibitor gene expression. PLoS One 2020;15 e0234691.

Jiang W, Wang Y, Tang J, Peng J, Wang Y, Guo Q, Guo Z, Li P, Xiao B, Zhang J. Low-intensity pulsed ultrasound treatment improved the rate of autograft peripheral nerve regeneration in rat. Sci Rep 2016;6:22773.

Johnson EM, Jr, Taniuchi M, DiStefano PS. Expression and possible function of nerve growth factor receptors on Schwann cells. Trends Neurosci 1988;11:299–304.

Khanna A, Nelmes RTC, Gougoulias N, Maffulli N, Gray J. The effects of LIPUS on soft-tissue healing: A review of literature. Br Med Bull 2009;89:169–182.

Lee IC, Lo TL, Young TH, Li YC, Chen NG, Chen CH, Chang YC. Differentiation of neural stem/progenitor cells using low-intensity ultrasound. Ultrasound Med Biol 2014;40:2195–2206.

Menorca RMG, Fussell TS, Elfar JC. Nerve physiology: Mechanisms of injury and recovery. Hand Clin 2013;29:317–330.

Ni XJ, Wang XD, Zhao YH, Sun HL, Hu YM, Yao J, Wang Y. The effect of low-intensity ultrasound on brain-derived neurotropic factor expression in a rat sciatic nerve crushed injury model. Ultrasound Med Biol 2017;43:461–468.

Nishida Y, Yamada Y, Kanemaru H, Ohazama A, Maeda T, Seo K. Vascularization via activation of VEGF-VEGFR signaling is essential for peripheral nerve regeneration. Biomed Res 2018;39:287–294.

Pan B, Liu Y, Yan JY, Wang Y, Yao X, Zhou HX, Lu L, Kong XH, Feng SQ. Gene expression analysis at multiple time-points identifies key genes for nerve regeneration. Muscle Nerve 2017;55:373–383.

Peng DY, Reed-Maldonado AB, Lin GT, Xia SJ, Lue TF. Low-intensity pulsed ultrasound for regenerating peripheral nerves: Potential for penile nerve. Asian J Androl 2020;22:335–341.

Petruska JC, Mendell LM. The many functions of nerve growth factor: Multiple actions on nociceptors. Neurosci Lett 2004;361: 168–171.

Ren C, Chen X, Du N, Geng S, Hu Y, Liu X, Wu X, Lin Y, Bai X, Yin W, Cheng S, Yang L, Zhang Y. Low-intensity pulsed ultrasound promotes Schwann cell viability and proliferation via the GSK-3 β/β-catenin signaling pathway. Int J Biol Sci 2018;14:497–507.

Romano CL, Romano D, Logoluso N. Low-intensity pulsed ultrasound for the treatment of bone delayed union or nonunion: A review. Ultrasound Med Biol 2009;35:529–536.

Sato M, Motoyoshi M, Shinoda M, Iwata K, Shimizu N. Low-intensity pulsed ultrasound accelerates nerve regeneration following inferior alveolar nerve transection in rats. Eur J Oral Sci 2016;124:246–250.

Schuh C, Hausner T, Redl H. A therapeutic shock propels Schwann cells to proliferate in peripheral nerve injury. Brain Circ 2016;2:138.

Shindo T, Shimokawa H. Therapeutic angiogenesis with sound waves. Ann Vasc Dis 2020;13:116–125.

Su WS, Wu CH, Chen SF, Yang FY. Transcranial ultrasound stimulation promotes brain-derived neurotrophic factor and reduces apoptosis in a mouse model of traumatic brain injury. Brain Stimul 2017;10:1032–1041.

Sun W, Sun C, Lin H, Zhao H, Wang J, Ma H, Chen B, Xiao Z, Dai J. The effect of collagen-binding NGF-β on the promotion of sciatic nerve regeneration in a rat sciatic nerve crush injury model. Biomaterials 2009;30:4649–4656.

Tajino J, Ito A, Tanima M, Yamaguchi S, Iijima H, Nakahata A, Kiyan W, Aoyama T, Kuroki H. Three-dimensional motion analysis for comprehensive understanding of gait characteristics after sciatic nerve lesion in rodents. Sci Rep 2018;8:13585.

Unezaki S, Yoshii S, Mabuchi T, Saito A, Ito S. Effects of neurotrophic factors on nerve regeneration monitored by in vivo imaging in thy1-YFP transgenic mice. J Neurosci Methods 2009;178:308–315.

Walker JL, Evans JM, Meade P, Resig P, Sisken BF. Gait-stance duration as a measure of injury and recovery in the rat sciatic nerve model. J Neurosci Methods 1994;52:47–52.

Wang T, Id AI, Aoyama T, Nakahara R, Nakahata A. Functional evaluation outcomes correlate with histomorphometric changes in the rat sciatic nerve crush injury model: A comparison between sciatic functional index and kinematic analysis. PLoS One 2018;13:e0208985.

Wang T, Ito A, Tajino J, Kuroki H, Aoyama T. 3D kinematic analysis for the functional evaluation in the rat model of sciatic nerve crush injury. J Vis Exp 2020;156:e60267.

Warden SJ. A new direction for ultrasound therapy in sports medicine. Sports Med 2003;33:95–107.

Willand MP, Nguyen MA, Borschel GH, Gordon T. Electrical stimulation to promote peripheral nerve regeneration. Neurorehabil Neural Repair 2016;30:490–496.

Willett NJ, Boninger ML, Miller LJ, Alvarez L, Aoyama T, Bedoni M, Brix KA, Chisari C, Christ G, Dearth CL, Dyson-Hudson TA, Evans CH, Goldman SM, Gregory K, Gualerzi A, Hart J, Ito A, Kuroki H, Loghmani MT, Mack DL, Malanga GA, Noble-Haeusslein L, Pasquina P, Roche JA, Rose L, Stoddart MJ, Tajino J, Terzic C, Topp KS, Wagner WR, Warden SJ, Wolf SL, Xie H, Rando TA, Ambrosio F. Taking the next steps in regenerative rehabilitation: Establishment of a new interdisciplinary field. Arch Phys Med Rehabil 2020;101:917–923.

Xia B, Chen G, Zou Y, Yang L, Pan J, Lv Y. Low-intensity pulsed ultrasound combination with induced pluripotent stem cells-derived neural crest stem cells and growth differentiation factor 5 promotes sciatic nerve regeneration and functional recovery. J Tissue Eng Regen Med 2019;13:625–636.

Zhang H, Lin X, Wan H, Li JH, Li JM. Effect of low-intensity pulsed ultrasound on the expression of neurotrophin-3 and brain-derived neurotrophic factor in cultured Schwann cells. Microsurgery 2009;29:479–485.

Zhao L, Feng Y, Hu H, Shi A, Zhang L, Wan M. Low-intensity pulsed ultrasound enhances nerve growth factor-induced neurite outgrowth through mechanotransduction-mediated ERK1/2−CREB−Trx-1 signaling. Ultrasound Med Biol 2016;42:2914–2925.

Zhong W, Chen X, Jiang P, Wan JMF, Qin P, Yu ACH. Induction of endoplasmic reticulum stress by sonoporation: Linkage to mitochondria-mediated apoptosis initiation. Ultrasound Med Biol 2013;39:2382–2392.